ChemPubSoc
Europe

Check for updates

Coordination Cages

Boosting Luminescence of Planar-Fluorophore-Tagged Metal–Organic Cages Via Weak Supramolecular Interactions

Dong Luo+,[a] Mian Li+,[b] Xiao-Ping Zhou,*[a, b] and Dan Li*[a]

Abstract: A variety of planar organic fluorophores (R = phenyl, naphthalenyl, pyrenyl) and luminescence promotors (X = Cl, Br, I) were equipped, respectively, on the alternatively arranged vertices of cubic Zn^{II}-imidazolate cages through orthogonal subcomponent self-assembly. It was found that supramolecular interactions, especially weak C—H···X interactions, play a key role in activating an efficient radiative pathway, coupled with reduced nonradiative decay rate through metal coordination, therefore significantly boosting the emission quantum yields of the system. This finding provides a strategy that utilizes molecular geometry and supramolecular interactions to modulate the emission efficiency of luminescent cage-based materials.

Luminescent metal–organic cages (MOCs) have garnered increasing attention in the field of supramolecular chemistry,[1] embracing a trend of heightened complexity for self-assembled materials that require design from both molecular and supramolecular levels.[2–6] Recently, some elegant systems involving organic fluorophores[2–4] and/or ligand-based charge transfer[2b, 5c] have been developed. For example, Nitschke and co-workers demonstrated typical organic fluorophores, such as pyrene, can be installed on the vertices of a tetrahedral M_4L_6 cage through subcomponent self-assembly (i.e., simultaneously forming C=N dynamic imine and M←N coordination bonds).[2a] In contrast, the highly emissive metallacages, reported by Stang and co-workers, have taken advantage of intrinsic aggregation-induced emission (AIE) behavior of the tetraphenylethylene moiety to boost their emission efficiency in aggregated or solid states.[3a]

A variety of design strategies have been proposed to boost solid-state emission in the broader fields of luminescent organic and metal-coordination compounds.[1b,7] In particular, noncovalent interactions, such as hydrogen, halogen, or metallophilic bonding, have been introduced to modulate or amplify luminescence of light-emitting materials.[6,8,9] A successful case reported recently utilizes intermolecular halogen bonding to enhance the luminescence of a simple platinum cyclometalated complex.[8a] The use of other halogen-related interactions[10] has also been demonstrated for a number of organic solid-state chromophores, which is shown to be very effective in regulating their photophysical behavior.[8b–e]

The incorporation of organic fluorophores into MOCs does not only induce rigidification effect through metal complexation,[11] but also offers an opportunity for designing add-on sites on the vertices or edges of the targeted nanoscale polyhedra (i.e., spatial effect). Both effects may contribute to the enhancement of emission intensity[8,11] and, moreover, the predefined spatial arrangement of chromophores facilitates the introduction of supramolecular interactions to modulate their luminescent properties.[8,9] Inspired by newly developed strategies to achieve fluorescence enhancement of mononuclear or dinuclear metal complexes,[8a,11] we seek to introduce noncovalent interactions to regulate the luminescence behavior of our metal-imidazolate cages,[12] which were obtained through orthogonal subcomponent self-assembly.[1c,13]

Previously we found that R-substituted benzylamine, aldehyde imidazole and transition metal could serve as subcomponents to construct several MOCs through orthogonal dynamic imine and coordination bonds.[12a] In the presence of halogen anions, it would favor the formation of cubic-like M_8L_{12} cages which possess both tetrahedral and octahedral metal centers (Scheme 1).[12b–d] In the present work, we report a family of self-assembled $Zn_8L_{12}X_4$ cages integrated with both organic fluorophores (R-sites) and luminescence promotors (X-sites), which are coupled via supramolecular interactions.[8c–e,14]
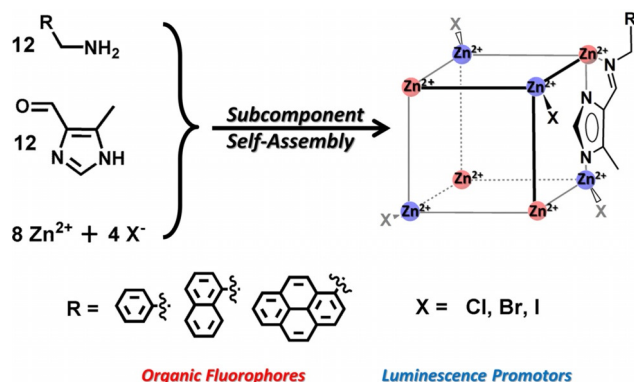
There are three aspects of rational considerations for the self-assembly of these luminescent cages. 1) The planar organic moieties (R = phenyl, naphthalenyl, pyrenyl) can be introduced through dynamic imine bonds, while the terminal halogen sites (X = Cl, Br, I) are attached via Zn←X coordination bonds, without interference to each other in the self-assembly. 2) Concerning the cage geometry, the R-substituted sites always reside beside the octahedral metal nodes, relative to the X-sites at the tetrahedral nodes, adopting an alternating arrangement at the vertices of the cube. The intruding X-sites can endow various noncovalent interactions for forming supramolecular networks.[10] 3) The simultaneous incorporation of multiple photophysically active subcomponents, that is, d^{10}-Zn^{II}

[a] D. Luo,+ Prof. X.-P. Zhou, Prof. D. Li
College of Chemistry and Materials Science, Jinan University
Guangzhou 510632 (P. R. China)
E-mail: danli@jnu.edu.cn

[b] M. Li,+ Prof. X.-P. Zhou
Department of Chemistry, Shantou University
Guangdong 515063 (P. R. China)
E-mail: zhouxp@stu.edu.cn

[+] These authors contributed equally to this work.

Supporting information and the ORCID identification numbers for the authors of this article can be found under https://doi.org/10.1002/chem.201800243.

Scheme 1. Illustration of subcomponent self-assembly of neutral, cubic Zn^{II}-imidazolate cages immobilized with planar organic fluorophores (R) and luminescence promotors (X) on the vertices.

ions, planar organic fluorophores (R) and efficient luminescence promotors (X),[8a,b, 15] warrants a systematical study on the emissive performance by varying the R and X sites.

This family of neutral, cubic $Zn_8L_{12}X_4$ cages (HL = N-((5-methyl-1H-imidazol-4-yl)methylene)R-methanamine, where R = phenyl for **1-X**, naphthalenyl for **2-X**, pyrenyl for **3-X**; X = Cl, Br, I) were constructed from the multicomponent reactions of 5-methyl-4-formylimidazole, R-substituted amines and ZnX_2 (see the Supporting Information for the Experimental Section).[12b–d] The solid-state samples of all the cages can be prepared easily with appreciable yields and have limited solubility in common organic solvents (e.g., EtOH, THF, DMF or DMSO). Except for **3-X**, six single-crystal structures of the MOCs (i.e., **1-X** and **2-X**) were determined (see the Supporting Information for crystal data).

To investigate the luminescence behavior of this system, we measured the UV/Vis absorption and excitation/emission spectra of the ligands and cages (Figure 1, see also Figures S5 and S6 in Supporting Information). In the concentration-varied emission spectra of the ligands (Figure 1a), one can clearly observe the high-energy, narrow bands (λ_{em} = 410–430 nm) attributed to the organic fluorophores, while the low-energy, broad bands (λ_{em} = 470–480 nm) emerge gradually at high con-
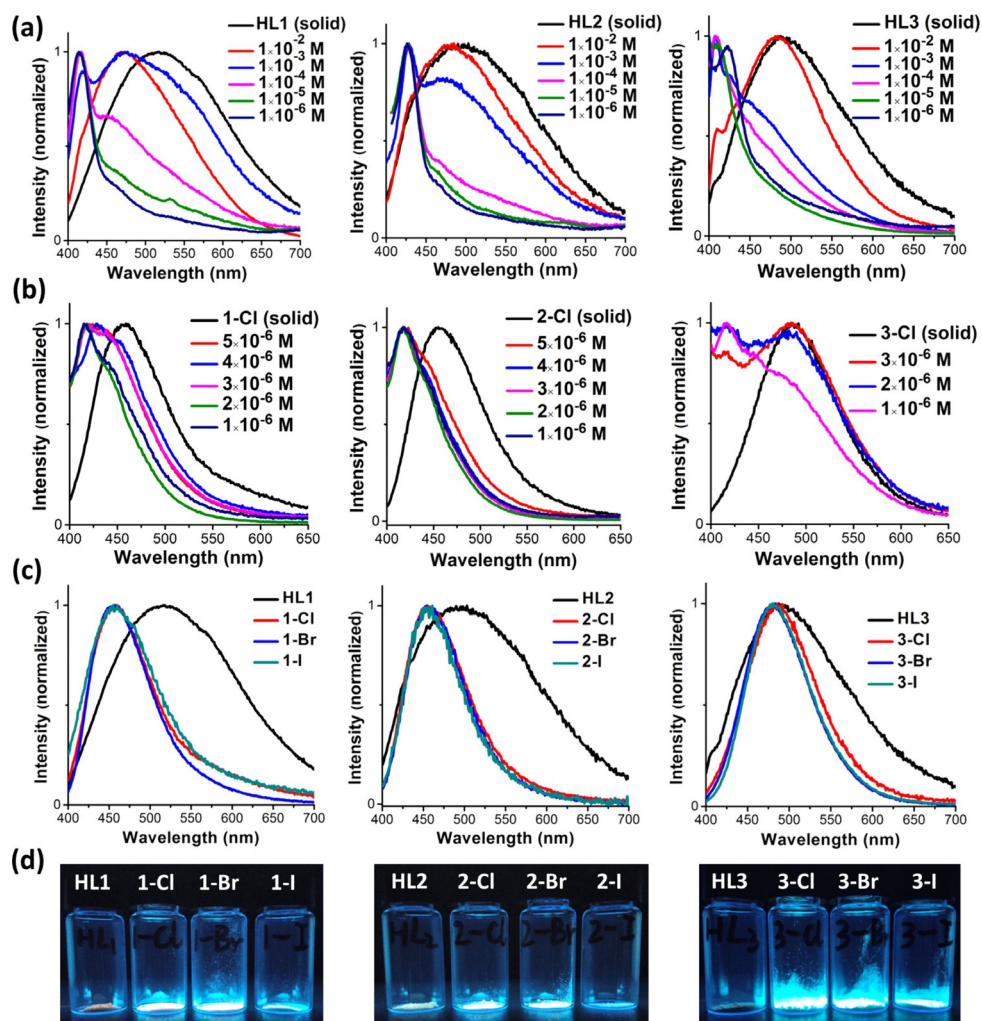
Figure 1. Comparison of emission spectra of: a) ligands HL1 to HL3, and b) cages **1-Cl** to **3-Cl** in THF solution with varied concentrations and in solid state. c) Solid-state emission spectra, and d) photographs of solid samples under UV light (365 nm excitation, room temperature) of all ligands and cages obtained. See Table 1 below for corresponding excitation wavelengths.

centrations and finally dominate for all the cases. These are due to the formation of excimers in aggregated states, which is commonly observed for planar fluorophores and would lower the emission intensity because of aggregation-caused quenching (ACQ).[7a,b] In the solid state, the broad bands are further red-shifted ($\lambda_{em} = 490\text{–}520$ nm) because of dense crystal packing, which would strengthen the intermolecular interactions between fluorophores. We have obtained the single-crystal structures of HL1 and HL2, confirming the existence of intermolecular $\pi\cdots\pi$, C–H$\cdots\pi$ and N–H$\cdots$N interactions (Figure S4 in Supporting Information). As a result, the solid samples of HL1 to HL3 are weakly emissive under UV light, compared with their cage analogues (Figure 1 d).

Due to their limited solubility, the solution-state emission of the cages can only be measured at low concentrations (ca. 10^{-6} M, Figure 1 b). For **1-Cl**, **2-Cl** and **3-Cl**, the high-energy bands ascribed to the organic fluorophore monomer still remain, whereas the low-energy bands now appear as shoulders. Note that their solid-state emission peaks ($\lambda_{em} = 450\text{–}480$ nm) shift towards higher energy relative to those of HL1 to HL3 (Figure 1 c), suggesting that the origin of emission for the cages may be different. This is supported by comparing the UV/Vis absorption and excitation spectra of ligands and cages, which differ significantly (Figure S5 in Supporting Information). We speculate either metal coordination or supramolecular interactions (or the combination of both) can contribute to such spectral alternations (see below for further discussion).

To verify the role of supramolecular interactions among cages, we examined the single-crystal structures of **1-X** and **2-X** carefully. **1-Cl**, **1-Br** and **1-I** are isostructures (cubic $I\bar{4}3m$), while **2-Cl/2-Br** (triclinic $P\bar{1}$) and **2-I** (monoclinic $C2/c$) crystallize in different space groups. Despite different crystal packing, there exist similar types of weak supramolecular contacts, that is, C–H$\cdots$X and $\pi\cdots\pi$ interactions, in the crystal structures of **1-X** and **2-X** (Figure 2 and Figure S3 in the Supporting Information). Taking **1-Cl** and **2-Cl** as examples, there are both intra- and intermolecular C–H$\cdots$X interactions (i.e., X–R contacts), similar to previous reports on several co-crystals involving weak halogen-related interactions between halogens and aromatic fluorophores.[14] Here the multiple, weak supramolecular interactions act together to fix the spatial arrangement of the organic fluorophores surrounding the vertices of the cubic cages in the solid state. Although the crystal structures of **3-X** cannot be determined due to poor crystallinity (Figures S14 and S15 in Supporting Information), it is likely that halogens also play an important role therein, given that they exhibit spectral shifting and enhanced luminescence similar to the situation for **1-X** and **2-X** (Figure 1).

In order to clarify the influences of metal–ligand coordination and weak supramolecular interactions on the luminescence behavior, we prepared mononuclear complexes, $[Zn(HL2)_3](NO_3)_2$ and $[Zn(HL2)_3]Cl_2$, and compared their emission spectra with that of HL2 and **2-Cl** (Figure S19 in Supporting Information). The emission peaks for the two mononuclear complexes are very close to that for HL2, other than **2-Cl**. This means that the coordination to zinc would not induce spectral shifting as in the case of **2-Cl**; it is the X–R contacts that are mainly responsible for the emission origin of the cages in the solid state.
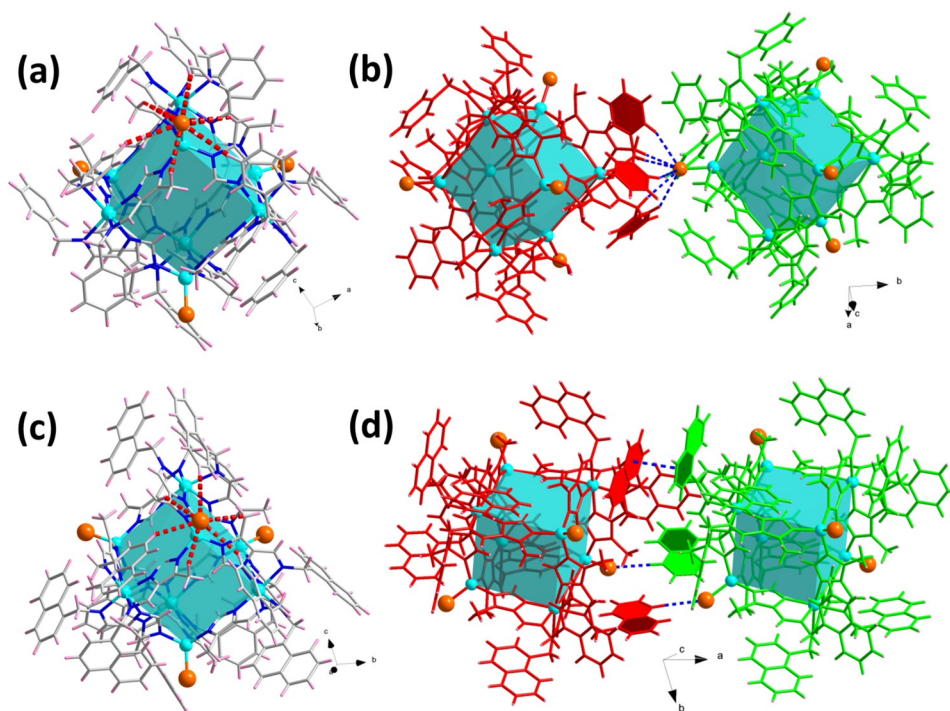
Figure 2. Structural diagrams showing the intra- (left, shown in red dashed lines) and intermolecular (right, shown in blue dashed lines) interactions in **1-Cl** (a, b) and **2-Cl** (c, d). Color codes: a,c) Zn, cyan; C, grey; N, blue; Cl, orange; H, pink. The cyan cubes highlight the geometry of the cage compounds. Color codes: b,d) two adjacent cages are colored in red and green, respectively.
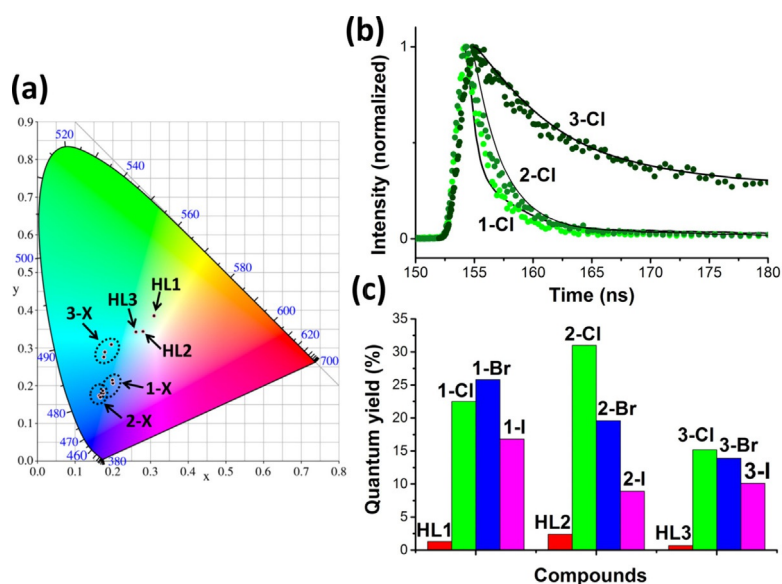
Figure 3. a) Luminescence colors shown in CIE 1931 chromaticity coordinates, b) fluorescence decay lifetime fitting, and c) emission quantum yields of the luminescent solid-state materials.

In the literature, the origin of solid-state luminescence involving halogen-related interactions was ascribed to an excimer/exciplex mechanism (which usually gives fluorescence)[8d,e] or heavy-atom effect (which usually gives phosphorescence).[14] However, these works suffered from the drawback of reduced luminescent efficiency compared with the parent fluorophores. We measured the emission decay of the solid samples (Figure 3b and Figures S10–S12 in the Supporting Information). The lifetimes at nanosecond scale indicate a fluorescence nature (Table 1 and Table S5 in the Supporting Information), ruling out the heavy-atom effect of halogens on producing phosphorescence through spin-orbital coupling.[8b,d,e]

Note that for **1-X** and **2-X** the lifetime data can adapt to biexponential fitting, ascribed to the excited fluorophore R* and exciplex (X–R)*, respectively, while **3-X** has a monoexponential decay possibly corresponding to excitation of excimer/exciplex (Table S5 in the Supporting Information). Therefore, the emissive-state decay of **3-Cl** is much slower than that of **1-Cl** and **2-Cl** (Figure 3b). This is also associated with the fact that the emission maxima for **1-X** and **2-X** are strongly blue shifted compared with the corresponding ligand, while it remains similar in the case of **3-X** (Figure 1c). Meanwhile, the dual emissions in solution (Figure 1) and largely unaltered peaks in the excitation-energy-varied emission spectra in the solid state (Figures S7–S9 in the Supporting Information) also support the assignment of origin to intermolecular exciplex-type states.

The emission color profiles of all the materials reported here are marked in the chromaticity coordinates shown in Figure 3a, which correspond to the solid-state emission spectra given in Figure 1c with blue to cyan luminescence for $Zn_8L_{12}X_4$ cages. Remarkably, the solid-state fluorescence of the cages is much brighter than that of the ligands (Figure 1d). Usually for planar organic fluorophores, the emission tends to be weakened or even quenched in the solid state, owing to the formation of excimer/exciplex (i.e., showing ACQ effect).[7a,b] In contrast, here the solid-state emission quantum yields of the cages exhibit four- to 20-fold increases relative to those of the ligands due to the X–R contacts (Figure 3c and Table 1). The emission maxima of the cages ($\lambda_{ex} = 456$ nm for **1-X** and **2-X**; 480 nm for **3-X**) are largely independent on the variation of the X-sites, but the introduction of halogens can give rise to much stronger luminescence and the emission efficiency can be tuned through varying halogens.

We calculated the radiative and nonradiative decay rate constants (k_r and k_{nr}) from the photophysical data (Table 1). The k_r

Table 1. Summary of photophysical parameters for the ligands and cages in the solid state at 298 K.

	λ_{em} [nm]	Φ[d]	$<\tau>$[e] [ns]	k_r[f] (10^7 s^{-1})	k_{nr}[g] (10^8 s^{-1})
HL1[a]	518	0.013	0.36	3.6	27.4
1-Cl[a]	456	0.225	1.88	12.0	4.1
1-Br[a]	456	0.258	1.17	22.1	6.3
1-I[a]	456	0.168	1.34	12.5	6.2
HL2[b]	495	0.024	0.54	4.4	18.1
2-Cl[b]	456	0.310	2.04	15.2	3.4
2-Br[b]	456	0.196	0.88	22.3	9.1
2-I[b]	456	0.089	0.57	15.6	16.0
HL3[c]	490	0.007	0.42	1.7	23.6
3-Cl[c]	480	0.152	6.75	2.3	1.3
3-Br[c]	480	0.139	6.41	2.2	1.3
3-I[c]	480	0.101	6.68	1.5	1.4

[a] $\lambda_{ex} = 370$ nm. [b] $\lambda_{ex} = 380$ nm. [c] $\lambda_{ex} = 380$ nm. [d] Absolute emission quantum yield ± 0.005. [e] $<\tau> = 1/(\alpha_1/\tau_1 + \alpha_2/\tau_2)$. [f] $k_r = \Phi/<\tau>$. [g] $k_{nr} = (1-\Phi)/<\tau>$. τ_1 and τ_2 are given in Table S5 in the Supporting Information.

values for all compounds lie at 10^7 s^{-1} scale, affirming the fluorescence nature (typically 10^5 s$^{-1} < k_r < 10^9$ s^{-1}).[15] For **1-X** and **2-X**, both the increased k_r and decreased k_{nr} values (compared with those of HL1 and HL2) contribute to the strong fluorescence, while for **3-X**, the significantly suppressed nonradiative decay is decisive for fluorescence enhancement. These are in agreement with the spectral assignment and lifetime fitting above. In addition, we measured and calculated the k_r and k_{nr} values for the mononuclear [Zn(HL2)$_3$](NO$_3$)$_2$ and [Zn(HL2)$_3$]Cl$_2$ (Table S6 in the Supporting Information). By comparison with that of HL2 and **2-Cl**, one can conclude that the role of metal coordination is mainly to reduce the nonradiative decay rate; however, the emission intensity of the mononuclear complexes is moderate ($\Phi = 0.075$ and 0.027, respectively), merely close to that of the ligand. Therefore, supramolecular interaction, especially weak C−H···X interactions, is a more important factor on boosting luminescence, which serves to activate an efficient radiative decay pathway.

Taken together, we demonstrate a modular approach, by utilizing orthogonal subcomponent self-assembly, to immobilize both planar organic fluorophores (R-sites) and luminescence promotors (X-sites) on the vertices of a family of cubic Zn$_8$L$_{12}$X$_4$ MOCs. The boosted luminescence intensity for the cage compounds in the solid state is mainly attributed to: 1) the increase of radiative decay rate constant via supramolecular interactions (X−R contacts) which induce the formation of exciplex-type states, and 2) the reduction of nonradiative deactivation pathways through metal coordination which can give rise to rigidification effect. This work provides a way to overcome the quenching effect of planar fluorophores in the solid state; more importantly, it represents a successful example of designing luminescent cage-based materials in respect of molecular geometry and supramolecular interactions, which fulfills the heightened requirement on integrating multiple levels of complexity for light-emitting materials design.

Acknowledgements

Conflict of interest

The authors declare no conflict of interest.

[1] a) T. R. Cook, P. J. Stang, Chem. Rev. **2015**, 115, 7001; b) V. W.-W. Yam, V. K.-M. Au, S. Y.-L. Leung, Chem. Rev. **2015**, 115, 7589; c) A. J. McConnell, C. S. Wood, P. P. Neelakandan, J. R. Nitschke, Chem. Rev. **2015**, 115, 7729; d) M. W. Cooke, G. S. Hanan, Chem. Soc. Rev. **2007**, 36, 1466; e) M. D. Ward, P. R. Raithby, Chem. Soc. Rev. **2013**, 42, 1619; f) P. D. Frischmann, K. Mahata, F. Würthner, Chem. Soc. Rev. **2013**, 42, 1847.

[2] a) P. P. Neelakandan, A. Jimenez, J. R. Nitschke, Chem. Sci. **2014**, 5, 908; b) A. J. Musser, P. P. Neelakandan, J. M. Richter, H. Mori, R. H. Friend, J. R. Nitschke, J. Am. Chem. Soc. **2017**, 139, 12050.

[3] a) X. Yan, T. R. Cook, P. Wang, F. Huang, P. J. Stang, Nat. Chem. **2015**, 7, 342; b) M. L. Saha, X. Yan, P. J. Stang, Acc. Chem. Res. **2016**, 49, 2527; c) M. Zhang, M. L. Saha, M. Wang, Z. Zhou, B. Song, C. Lu, X. Yan, X. Li, F. Huang, S. Yin, P. J. Stang, J. Am. Chem. Soc. **2017**, 139, 5067.

[4] a) F. Würthner, C.-C. You, C. R. Saha-Moller, Chem. Soc. Rev. **2004**, 33, 133; b) P. D. Frischmann, V. Kunz, F. Würthner, Angew. Chem. Int. Ed. **2015**, 54, 7285; Angew. Chem. **2015**, 127, 7393; c) P. D. Frischmann, V. Kunz, V. Stepanenko, F. Würthner, Chem. Eur. J. **2015**, 21, 2766; d) M. Yoshizawa, J. K. Klosterman, Chem. Soc. Rev. **2014**, 43, 1885; e) Y. Okazawa, K. Kondo, M. Akita, M. Yoshizawa, J. Am. Chem. Soc. **2015**, 137, 98; f) M. Yoshizawa, M. Yamashina, Chem. Lett. **2017**, 46, 163; g) L. Xu, Y.-X. Wang, H.-B. Yang, Dalton Trans. **2015**, 44, 867; h) J. Wang, C. He, P. Wu, J. Wang, C. Duan, J. Am. Chem. Soc. **2011**, 133, 12402; i) L. Yang, X. Jing, C. He, Z. Chang, C. Duan, Chem. Eur. J. **2016**, 22, 18107; j) D. R. Martir, D. Escudero, D. Jacquemin, D. B. Cordes, A. M. Z. Slawin, H. A. Fruchtl, S. L. Warriner, E. Zysman-Colman, Chem. Eur. J. **2017**, 23, 14358.

[5] a) L.-L. Yan, C.-H. Tan, G.-L. Zhang, L.-P. Zhou, J.-C. Bünzli, Q.-F. Sun, J. Am. Chem. Soc. **2015**, 137, 8550; b) X.-Z. Li, L.-P. Zhou, L.-L. Yan, D.-Q. Yuan, C.-S. Lin, Q.-F. Sun, J. Am. Chem. Soc. **2017**, 139, 8237; c) C.-L. Liu, R.-L. Zhang, C.-S. Lin, L.-P. Zhou, L.-X. Cai, J.-T. Kong, S.-Q. Yang, K.-L. Han, Q.-F. Sun, J. Am. Chem. Soc. **2017**, 139, 12474.

[6] a) G.-F. Gao, M. Li, S.-Z. Zhan, Z. Lv, G.-H. Chen, D. Li, Chem. Eur. J. **2011**, 17, 4113; b) J.-H. Wang, M. Li, J. Zheng, X.-C. Huang, D. Li, Chem. Commun. **2014**, 50, 9115.

[7] a) J. Mei, N. L. C. Leung, R. T. K. Kwok, J. W. Y. Lam, B. Z. Tang, Chem. Rev. **2015**, 115, 11718; b) Q. Li, Z. Li, Adv. Sci. **2017**, 4, 1600484; c) S. Hirata, Adv. Opt. Mater. **2017**, 5, 1700116; d) L. Ravotto, P. Ceroni, Coord. Chem. Rev. **2017**, 346, 62.

[8] a) V. V. Sivchik, A. I. Solomatina, Y.-T. Chen, A. J. Karttunen, S. P. Tunik, P.-T. Chou, I. O. Koshevoy, Angew. Chem. Int. Ed. **2015**, 54, 14057; Angew. Chem. **2015**, 127, 14263; b) O. Bolton, K. Lee, H.-J. Kim, K. Y. Lin, J. Kim, Nat. Chem. **2011**, 3, 205; c) U. Mayerhöffer, F. Würthner, Angew. Chem. Int. Ed. **2012**, 51, 5615; Angew. Chem. **2012**, 124, 5713; d) D. Yan, A. Delori, G. O. Lloyd, T. Friscic, G. M. Day, W. Jones, J. Lu, M. Wei, D. G. Evans, X. Duan, Angew. Chem. Int. Ed. **2011**, 50, 12483; Angew. Chem. **2011**, 123, 12691; e) D. Yan, D.-K. Bucar, A. Delori, B. Patel, G. O. Lloyd, W. Jones, X. Duan, Chem. Eur. J. **2013**, 19, 8213.

[9] a) Z. Zhao, P. Lu, J. W. Y. Lam, Z. Wang, C. Y. K. Chan, H. H. Y. Sung, I. D. Williams, Y. Ma, B. Z. Tang, Chem. Sci. **2011**, 2, 672; b) Y. Gong, G. Chen, Q. Peng, W. Z. Yuan, Y. Xie, S. Li, Y. Zhang, B. Z. Tang, Adv. Mater. **2015**, 27, 6195; c) Z. He, W. Zhao, J. W. Y. Lam, Q. Peng, H. Ma, G. Liang, Z. Shuai, B. Z. Tang, Nat. Commun. **2017**, 8, 416; d) J. Yang, Z. Ren, Z. Xie, Y. Liu, C. Wang, Y. Xie, Q. Peng, B. Xu, W. Tian, F. Zhang, Z. Chi, Q. Li, Z. Li, Angew. Chem. Int. Ed. **2017**, 56, 880; Angew. Chem. **2017**, 129, 898.

[10] a) L. C. Gilday, S. W. Robinson, T. A. Barendt, M. J. Langton, B. R. Mullaney, P. D. Beer, Chem. Rev. **2015**, 115, 7118; b) B. Li, S.-Q. Zang, L.-Y. Wang, T. C. W. Mak, Coord. Chem. Rev. **2016**, 308, 1; c) G. R. Desiraju, P. S. Ho, L. Kloo, A. C. Legon, R. Marquardt, P. Metrangolo, P. Politzer, G. Resnati, K. Rissanen, Pure Appl. Chem. **2013**, 85, 1711; d) X.-L. Wang, J. Zheng, M. Li, S. W. Ng, S. L.-F. Chan, D. Li, Cryst. Growth Des. **2016**, 16, 4991.

[11] N. Sinha, L. Stegemann, T. T. Y. Tan, N. L. Doltsinis, C. A. Strassert, F. E. Hahn, Angew. Chem. Int. Ed. **2017**, 56, 2785; Angew. Chem. **2017**, 129, 2829.

[12] a) X.-P. Zhou, J. Liu, S.-Z. Zhan, J.-R. Yang, D. Li, K.-M. Ng, R. W.-Y. Sun, C.-M. Che, J. Am. Chem. Soc. **2012**, 134, 8042; b) X.-P. Zhou, Y. Wu, D. Li, J. Am. Chem. Soc. **2013**, 135, 16062; c) D. Luo, X.-P. Zhou, D. Li, Angew. Chem. Int. Ed. **2015**, 54, 6190; Angew. Chem. **2015**, 127, 6288; d) D. Luo, X.-P. Zhou, D. Li, Inorg. Chem. **2015**, 54, 10822.

[13] a) V. Goral, M. I. Nelen, A. V. Eliseev, J.-M. Lehn, Proc. Natl. Acad. Sci. USA **2001**, 98, 1347; b) J. R. Nitschke, Acc. Chem. Res. **2007**, 40, 103; c) T. K. Ronson, S. Zarra, S. P. Black, J. R. Nitschke, Chem. Commun. **2013**, 49, 2476; d) A. M. Castilla, W. J. Ramsay, J. R. Nitschke, Acc. Chem. Res. **2014**, 47, 2063.

[14] a) Q. J. Shen, X. Pang, X. R. Zhao, H. Y. Gao, H.-L. Sun, W. J. Jin, *CrystEng-Comm* **2012**, *14*, 5027; b) S. d'Agostino, F. Grepioni, D. Braga, B. Ventura, *Cryst. Growth Des.* **2015**, *15*, 2039.

[15] N. J. Turro, V. Ramamurthy, J. C. Scaiano, *Modern Molecular Photochemistry of Organic Molecules*, Chemical Industry Press, Beijing, **2015**.